PHYSICAL REVIEW VOLUME 188, NUMBER 1 5 DECEMBER 1969

Theory of Melting Helium-3 at Very Low Temperatures

Louis Goldstein

University of California, Los Alamos Scientific Laboratory, Los Alamos, New Mexico 87544

(Received 28 April 1969)

In earlier work, we obtained the higher-temperature melting properties of He^3 with the solid in the paramagnetic range. The exchange-coupled solid was assumed to become antiferromagnetic below its spin-ordering temperature. The thermal excitations of the permanently paramagnetic liquid were described in terms of its spin and nonspin degrees of freedom according to a theory of this phase elaborated in early work. Recent accurate measurements of the melting properties of He^3 permit a critical comparison of theory with experiment. With complete spin disorder in the solid at melting, at even the lowest temperature reached in the measurements, the latter confirm the satisfactory accuracy of the theoretical entropy of the liquid at melting. We now use the asymptotic molecular-field-theory model to extend the description of melting He^3 into the antiferromagnetic range of the solid. The effect of the magnetic transition at melting allows one to locate the temperature at which this transformation begins. The low temperatures attained by adiabatic freezing, which we studied previously, are shown to have a theoretical lower limit of about 0.5 m°K. This is identical with the low-temperature maximum of the melting pressure or the end of the anomalous melting phenomenon which starts at the melting-pressure minimum around 325 m°K. The characteristic cooling on adiabatic freezing over the indicated temperature range is, nevertheless, far from exhausting the physical content of the remarkable melting anomaly of He^3. It is thus proved that the cooling effect permits the verification of the theoretical melting pressure down to the upper reaches of its indicated low-temperature limit. This is shown to be feasible without the measurements of the still unknown very low temperatures. This verification procedure determines the latter unambiguously through the intermediary of the entropies of the liquid and solid at melting; the functional arguments of the accurately measured melting pressure changes between initial and final states of the adiabatic freezing process. A thermodynamic standard of temperatures, down to very low temperatures, has been obtained thereby. This should open up a new field of experimental investigations where, heretofore, in the absence of its direct and accurate accessibility, the concept of temperature seemed to lose some of its significance. The thermodynamic He^3 melting-pressure thermometry, at the very low temperatures, may reasonably be expected to initiate and guide the charting of the submillidegree range, which at the present time and on the basis of the results obtained in the present work becomes accessible only by magnetic cooling.

I. INTRODUCTION

Our recent work[1] on solid He^3 was restricted to that temperature range where this solid exhibits nuclear paramagnetism. This limitation could be justified on the following grounds. With the possible exception of a small temperature interval of a few hundredths of a millidegree absolute above the spin-ordering temperature of the solid, its thermal properties could be calculated exactly in terms of an assumed interatomic coupling model. The mutual potential energy of atomic pairs was taken to be proportional to the scalar product of the nuclear-spin vectors on nearest neighbors. The technical difficulties arising from accurate measurements of very low temperatures also tended to restrict the useful temperature range where thermal-property data of acceptable accuracy and precision could be produced. Furthermore, no exact theoretical models are, at the present time, available for the treatment of solid He^3 below its expected spin-ordering temperature at and below melting volumes or at and above melting pressures. More recently, it appeared to be of interest to follow solid He^3 from its empirically estimated transition temperature, at melting, down toward the absolute zero, through the approximate treatments provided by simple asymptotic spin-ordering models. This is one of the main topics of the present paper. Namely, the various very low-temperature thermal properties of solid He^3, the melting pressure included, will be evaluated here within the limitations of the molecular-field-theory formalism involving only the empirically determined equilibrium-exchange-energy coupling parameter of the solid at melting. This was determined experimentally by Adams and his collaborators.[2] The approximate transition or spin-ordering temperature at melting results from an empirical rule

which has only numerical justification. This rule appears to represent, to some degree of numerical approximation, the very much higher transition temperatures of ferromagnetic and antiferromagnetic ionic or electronic systems.[3]

In our approach, the exact if incomplete theoretical description of the paramagnetic solid, with the assumed exchange-coupling scheme, has to be joined at the spin-ordering or transition temperatures to the approximate molecular-field-theory formalism restricted to the spin-ordering range of the thermodynamic variables of state. At melting, continuity of the melting pressure and its temperature derivative is achieved through requiring continuity of the entropy and volume of the solid at the transition point. Above melting in the compressed solid, the study of which is reserved for later work, the continuity of the entropy at the transition line would insure that of the pressure along the isochores of the solid. The derivative thermal properties are, however, discontinuous both at melting and above it along the transition line. This state of affairs may well be compatible with the approximate theoretical derivative thermal properties somewhat below and with their exact representation somewhat above the transition temperature at melting or above the transition line. Over a temperature range of a few hundredths of a millidegree absolute below and above the transition temperature, the present approach may break down, as far as the derivative thermal properties are concerned. Critical behavior, if present, would be expected to become acute only over the indicated small temperature range. Its consideration and discussion is omitted in this paper.

At melting, the situation referring to He^3 is a particular case of the following problem. Given a first-order phase-transformation process wherein one of the two phases undergoes a higher-order phase change from a disordered into an ordered state, the phase-boundary line is modified by the intraphase higher-order transformation, the details of which may, in general, be ascertained through the analysis of the phase-boundary line. We will digress briefly in connection with this problem to discuss the saturation vapor-pressure and the melting-pressure lines of He^4 around their respective λ points. The location of the spin-ordering temperature (as in He^3), or of the higher-order transition points, (as in He^4), can in principle be determined through direct measurements of the temperature derivatives of the phase-boundary line. In the He^4 case though, this approach appears to be successful only at melting and not at the vapor-liquid phase-boundary line as a consequence of the anomalous behavior of the vapor along this line.

Pursuant to recent work at not-too-low temperatures, [1] we investigate in detail the full temperature range available through the cooling process which accompanies the adiabatic freezing of He^3. The approximate molecular-field-theory model of the assumed antiferromagnetic solid in the spin-ordering range leads to the location of the lowest temperature attainable through adiabatic solidification of He^3. It may be presumed that models other than the one used here for the spin-ordering solid should lead to some similar lower limit of the coldest temperature accessible through the above process. However, the practical lower limits are expected to be at considerably higher temperatures than the absolute theoretical lower limit.

The adiabatic freezing and cooling of He^3 will then be exploited along the following lines. On the one hand, these adiabatic processes should enable one to verify experimentally with accuracy the here-derived melting-pressure line, down to the lowest temperatures available practically through adiabatic freezing. On the other hand, the detailed analysis of the melting pressure of He^3 down to very low temperatures will be shown to open the possibility of He^3 melting-pressure thermometry. This in turn should lead to the establishment of thermodynamic temperature standards at very low temperatures, between about 10–15 and 1.0–1.5 m°K. The existence of such a thermodynamic standard at such low temperatures is of interest for accurate experimental investigations at these very low temperatures. In addition, it may become of significance in the charting of the submillidegree temperature interval, still considerably beyond the working temperature range close at hand at the present time.

II. MELTING He^3 ABOVE THE SPIN-ORDERING TEMPERATURE OF THE SOLID

In the limit of low-enough temperatures, the entropy expression of the liquid at melting, [1] $S_{L,M}(T)$, reduces to its asymptotic form linear in T. This entropy may be combined with the spin and phonon entropy of the solid at melting, both describable analytically within the limits of validity of the underlying models of these thermal excitations. This then yields an analytic expression for the temperature derivative of the melting pressure, $dP_M(T)/dT$, and for the melting-pressure changes $P_M(T_1) - P_M(T_2)$, as well as for the melting pressure itself, $P_M(T)$. At increasing temperatures, only the entropy of the solid is available in analytical form.[1] This was represented[1] by

$$S_{s,M}(T) = S_{M,\varphi}(T) + S_{M,m}(T), \tag{1}$$

on the reasonable assumption of the essential independence of the phonon entropy $S_{M,\varphi}$ and the

magnetic entropy $S_{M,m}$ arising from the assumed interatomic spin-dependent exchange-coupling scheme. The small phonon entropy when taken into account in earlier work was approximated by that of the asymptotic ideal phonon system. The magnetic entropy is associated with the interaction energy,

$$V_{ij} = -2J\vec{s}_i \cdot \vec{s}_j \quad , \tag{2}$$

of pairs of nearest-neighbor atoms i and j proportional to the scalar product of their spin vectors $\vec{s}$, J being the empirical exchange energy parameter which is strongly volume- or pressure-dependent. The residual temperature dependence of this parameter is expected to be small and will be omitted here. Beside the strictly magnetic approach, we have indicated earlier[1] several magneto-thermodynamic effects useful for the experimental verifications of the interspin couplings as well as the deduction of the sign of the parameter J. In Eq. (2), a positive J imposes ferromagnetic spin ordering, a negative J imposes antiferromagnetic spin ordering, in solid He^3. At the present time, we are unaware of any determinations of the sign of J, so that neither type of magnetic ordering can be ruled out. In the paramagnetic temperature range of the solid, the formalism can describe simultaneously either type of spin ordering. Accordingly, we will carry the notations of both types of spin ordering, although the numerical evaluations of the thermal properties of interest here will be limited to the antiferromagnetic solid. The similarity in the formalisms of the two spin-ordering processes in their paramagnetic range is connected with the exact, if incomplete, series representations of the magnetic and thermal properties of the exchange-coupled systems. These series proceed in ascending powers of the unique natural parameter available in the statistical thermodynamics of these systems, namely, $|J|/kT$ and $(-)|J|/kT$ in the ferromagnetic and antiferromagnetic configurations, respectively. As obtained earlier,[1] one has, using the superscripts (A), (F) for the two spin-ordering processes,

$$S_{M,m}^{(A),\,(F)}(x)/R = \ln 2 - 3\sum_{n=0} (\mp)^n (c_n/n+2)x^{n+2}, \quad x = |J|/kT \tag{3}$$

where the $(-)^n$ factors refer to antiferromagnetic ordering. Tables of the coefficients c_n are available[3] up to $n=5$ for the bcc solid under consideration. Additional coefficients up to $n=8$ are found in more recent work.[4]

The entropy of the liquid at melting was shown[1] to be described with fair accuracy by

$$S_{L,M}(T) = S_{L,M,\sigma}(T) + S_{L,M,n\sigma}(T) \quad . \tag{4}$$

with the component spin σ and nonspin $n\sigma$ entropies, In the limit of very low temperatures, it becomes justified to write[1]

$$\lim_{T \text{ small}} S_{L,M}(T)/R = \gamma T, \quad \gamma \cong 4.58/(^\circ\text{K}) \quad . \tag{5}$$

Both entropy components of (4) have been discussed in detail.[1,5] The coefficient γ takes into account approximately the anomalous increase in the entropy arising from the volume decrease of the liquid as a consequence of the melting-pressure increase, down to 5 m°K. Below this temperature the expected variations of the density or volume are likely to be small, and of negligible effect on the characteristic temperature $T_{0,\sigma}$ of the spin system of the liquid at melting. The treatment of the entropy $S_{L,M}(T)$ is far from exhaustive. The approximation used for the nonspin component $S_{L,M,n\sigma}(T)$ will improve as more extensive and accurate data become available on the thermal properties of the compressed liquid.

We have already considered[1] the limitations arising from the entropy [Eq. (3)] of the solid at melting, wherein an averaged $|J|$ value is assigned to the solid along the melting line, in spite of small variations of its volume and the ensuing changes in the $|J|$ values. As noted earlier,[1] improved theoretical values of the entropy of the assumed solid model should become available with extensive data on solid melting volumes in the relevant temperature range, $T < T_\mu$, T_μ being the temperature of the minimum of the He^3 melting pressure. From thermodynamics, the temperature derivative of the melting pressure $P_M(T)$ is

$$\frac{dP_M(T)}{dT} = \frac{S_{L,M}(T) - S_{s,M}(T)}{V_{L,M}(T) - V_{s,M}(T)} = \Delta S_M(T)/\Delta V_M(T) \quad . \tag{6}$$

In our previous work,[1] at $T < T_\mu$, we also assumed, in absence of pertinent data, that the volume change at melting, ΔV_M, was constant in a starting approximation. It was pointed out by Adams and his collaborators[6] that in spite of using an averaged $|J_M|$ value and a temperature-independent, and hence approximate, ΔV_M value, in contrast with the observed moderate variations of ΔV_M below T_μ, the measured melting-pressure changes were in agreement with those calculated by us.[1] The experimentally explored temperature range[6] extended between 17 and 318 m°K. The observation[6] of the increase of ΔV_M by about 5% of

its value at T_μ down to 60 m°K, approximately, and its subsequent slow decrease remain to be explained. The calculated melting pressures or, more exactly, the melting-pressure changes result from a straightforward integration of the derivative (6), defined, among others, by the theoretical entropy of the liquid at melting with the phenomenological constants entering into the component entropies $S_{L,M,\sigma}$ and $S_{L,M,n\sigma}$. Over the experimentally explored temperature range, the entropy of the solid at melting is found to be given, according to (3), by its asymptotic high-temperature limit of $(R\ln 2)$ to within less than $\frac{1}{2}\%$. It remains there unaffected, essentially, by the value of the exchange energy parameter $|J|$. Assuming that the measured melting-pressure variations are correct, within their experimental errors, the close agreement between the measurements and calculations over a relatively wide range of temperatures could come about as follows: In Eq. (6), the relative correction in $\Delta V_M^{(0)}$, the value used by us, is $\delta(\Delta V_M^{(0)})/\Delta V_M^{(0)}$. This must cancel the relative corrections of $\Delta S_M^{(0)}$, the theoretical entropy change at melting, or with

$$\Delta S_M(T) = \Delta S_M^{(0)}(T)[1 + \delta(\Delta S_M^{(0)})/\Delta S_M^{(0)}] \quad (7a)$$

and $$\Delta V_M(T) = \Delta V_M^{(0)}[1 + \delta(\Delta V_M^{(0)})/\Delta V_M^{(0)}], \quad (7b)$$

wherein $\delta(\Delta V_M^{(0)})$ is temperature-dependent, we have

$$dP_M(T)/dT = \frac{dP_M^{(0)}(T)}{dT} \frac{1 + \delta(\Delta S_M^{(0)})/\Delta S_M^{(0)}}{1 + \delta(\Delta V_M^{(0)})/\Delta V_M^{(0)}}, \quad (8)$$

for the exact melting-pressure derivative. The calculated melting-pressure changes resulting from $dP_M^{(0)}/dT$ may agree with the measured ones if

$$\delta(\Delta S_M^{(0)})/\Delta S_M^{(0)} \simeq \delta(\Delta V_M^{(0)})/\Delta V_M^{(0)}. \quad (9)$$

Over the explored temperature range, the solid entropy is almost constant at $R\ln 2$, and Eq. (9) is equivalent to

$$\delta(S_{L,M}^{(0)})/S_{L,M}^{(0)} \simeq \delta(\Delta V_M^{(0)})/\Delta V_M^{(0)}. \quad (10)$$

The entropy of the liquid given by Eq. (4) is thus slightly underestimated. It should be stressed again that values of $S_{L,M}(T)$ used in the calculations are approximate. Over a range of temperatures considered here, the liquid entropy becomes very small compared with the rapidly falling entropy of the solid, but in the limit of our lowest temperatures the two entropies again become comparable.

A detailed comparison of the calculated pressure changes, melting pressures, and derivatives $dP_M^{(0)}/dT$ with those deduced by the experimental workers[6] will be taken up later.

In recent work[1] we gave the equation of the melting-pressure line of He^3 from T_μ down to 5 m°K. The entropy contribution of the liquid had to be calculated because a valid analytical expression over the whole range of temperatures did not exist. With $\Delta V_M^{(0)}$ independent of the temperature, we rewrite the melting-pressure derivative as

$$dP_M^{(A),(F)}/dT = (1/\Delta V_M^{(0)})[S_{L,M}^{(0)}(T) - S_{M,m}^{(A),(F)}(x)], \quad (11)$$

$$x = |J_M|/kT .$$

Values of $S_{L,M}^{(0)}(T)$ were given in graphical form down to 5 m°K; the entropies $S_{M,m}^{(A),(F)}(T)$ are given by Eq. (3). It should be noted that we will neglect the very small phonon entropy of the solid in comparison with the entropy of its spin system throughout the temperature range considered. Then the melting-pressure changes resulting from Eq. (11), with (3), are

$$\Delta P_M^{(A),(F)}(x, x_\mu) = P_M^{(A),(F)}(x) - P_M^{(A),(F)}(x_\mu)$$
$$= (R/\Delta V_M^{(0)}) \int_{T_\mu}^{T} [S_{L,M}^{(0)}(T)/R]dT + (T_\mu - T)\ln 2 - [Q^{(A),(F)}(x) - Q^{(A),(F)}(x_\mu)] , \quad (12)$$

where $$Q^{(A),(F)}(z) = 3(|J_M|/k) \sum_{n=0} (\mp)^n [c_n/(n+1)(n+2)] z^{n+1}. \quad (13)$$

With $P_M(T_\mu)$ taken to be[7] 28.92 atm, we gave[1] a graph of $P_M(T)$, using 1.25 m°K for $|J_M|/k$, between 400 and 5 m°K. The melting line was then recalculated from an averaged value of $|J_M|/k = 0.7$ m°K, obtained from measurements made on the low-pressure solid by the Panczyk *et al.*[2] Some of our recalculated melting pressures were given by Adams and his coworkers[2] in a graph where the measured pressures were compared with the calculated ones below 80 m°K. The melting pressures were affected very

little over the experimentally explored temperature range by replacing the larger $|J_M|$ value with the smaller one. This is as expected, since, according to the melting-pressure expression (12), the contribution arising from the decrease of $S_{S,M}(T)$ below its asymptotic limit is negligible. However, the temperature of the inflection point of the melting line is lowered from about 10.5 to about 7 m°K reducing the value of $|J_M|/k$.

At temperatures below 5 m°K, one can use the asymptotic form of the liquid entropy [Eq. (5)] linear in T. The melting-pressure derivative becomes

$$dP_M^{(A),(F)}/dT = (R/\Delta V_M^{(0)})[\gamma T - S_{S,M}^{(A),(F)}(x)/R] \ , \tag{14}$$

where $T_0 \leq T \leq 5$ m°K and $S_{S,M}(x)$ are given by Eq. (3). Hence, over the same temperature range, the melting-pressure changes become

$$\Delta P_M^{(A),(F)}(x, x_\gamma) = P_M^{(A),(F)}(x) - P_M^{(A),(F)}(x_\gamma)$$

$$= (R/\Delta V_M^{(0)})\{\tfrac{1}{2}\gamma(T^2 - T_\gamma^2) + (T_\gamma - T)\ln 2 - [Q^{(A),(F)}(x) - Q^{(A),(F)}(x_\gamma)]\} \ , \tag{15}$$

where $x_\gamma = |J_M|/kT_\gamma$, $T_\gamma \leq 5$ m°K, and the Q function is defined through (13).

The transition temperatures of the solid at melting, $T_{O,M}(A)$ and $T_{O,M}(F)$, are the end points on the melting-line of the loci $T_0^{(A)}(V)$ and $T_0^{(F)}(V)$ of the spin-ordering temperatures of the low-pressure solid He^3. As noted in the Introduction, these loci are defined at the present time through strictly heuristic relations, such as[3]

$$T_0^{(A),(F)}(V) = \tau^{(A),(F)}|J(V)|/k \ ,$$
$$\tau^{(A)} \simeq 2.92, \quad \tau^{(F)} \simeq 2.64 \ . \tag{16}$$

At the larger solid volumes, the results[2] on $J(V)/k$ could be represented by the strictly empirical relation

$$J(V)V^{\Gamma_j} = \text{const}, \quad \Gamma_j = -16.4 \ . \tag{17}$$

According to recent work by Adams and Panczyk,[8] this relation overestimates the numerical value of $J(V)/k$ at the smaller volume of 21.5 cm^3/mole of the solid. These measurements extended the earlier ones[2] down to 13 m°K.

It may be appropriate at this point to compare the calculated melting pressures or pressure changes and pressure derivatives with the corresponding data of Adams and his collaborators.[6] These workers gave only a brief comparison of the melting data in their communication.[6] A more detailed comparison of the theoretical melting properties with their measured and deduced values is of interest, because the melting phenomenon of He^3 might possibly be used as a thermometric process resulting in a thermodynamic temperature scale at low temperatures. This pragmatic aspect of melting He^3 obviously requires a satisfactory theoretical representation of the melting pressure $P_M(T)$.

Listed in Table I are calculated values of the melting pressure $P_M(T)^{(a)}$; measured values $P_M(T)^{(b)}$ resulting from smoothed data of Scribner *et al.*[6]; and calculated melting-pressure changes $[P_M(T) - P_M(T_\mu)]^{(a)}$ at $T < T_\mu$ down to 5 m°K. These are the basic numerical results of the theory over the indicated temperature range. Indeed, the theoretical melting pressures themselves are obtained by accepting the empirical-state coordinates[7]

$$T_\mu \cong 326 \text{ m°K}, \quad P_M(T_\mu) = 28.92 \text{ atm},$$

and combining these reference data with the exactly calculated differences $[P_M(T) - P_M(T_\mu)]^{(a)}$. The differences $[P_M(T) - P_M(T_\mu)]^{(d)}$ result from the smoothed $P_M(T)^{(b)}$ data and the reference coordinates[6]

$$T_\mu = 318 \pm 5 \text{ m°K}, \quad P_M(T_\mu) = 28.94 \pm 0.03 \text{ atm}.$$

The direct comparison of the melting pressures themselves is somewhat misleading, since the basic theoretical values refer to melting-pressure changes. Also, the experimental melting pressures result from a combination of quite accurate melting-pressure changes with less accurate reference coordinates. Since the pressure changes were not published as such, the $[P_M(T) - P_M(T_\mu)]^{(d)}$ values of Table I are subject to large pressure uncertainties, ±0.03 atm. It is to be hoped that in the future, pressure changes will be given as the basic experimental data.

Within the accuracy of the reference pressure

TABLE I. He^3 melting pressures, melting pressure changes, and temperature derivatives at medium and low temperatures.

T	$P_M(T)$ [a]	$P_M(T)$ [b]	$[P_M(T)-P_M(T_\mu)]$ [a]	$[P_M(T)-P_M(T_\mu)]$ [c]	$(-)\left(\frac{dP_M}{dt}\right)$ [a]	$(-)\left(\frac{dP_M}{dt}\right)$ [d]
m°K		atm			atm/°K	
300	28.933		0.01310		1.192	
270	28.996		0.7561		2.382	
250	29.069	29.07	0.1490	0.13	4.324	4.1
230	29.170		0.2503		5.814	
210	29.303		0.3832		7.469	
200	29.382	29.36	0.4619	0.42	8.317	8.2
180	29.567		0.6474		10.286	
160	29.795		0.8746		12.473	
150	29.925	29.92	1.0052	0.98	13.649	14.2
140	30.068		1.1482		14.982	
130	30.225		1.3056		16.425	
120	30.397		1.4773		17.908	
110	30.585		1.6647		19.589	
100	30.789	30.80	1.8692	1.86	21.339	21.2
90	31.012		2.0922		23.239	
80	31.255	31.26	2.3349	2.32	25.357	24.6
70	31.519		2.5996		27.590	
60	31.807	31.80	2.8874	2.86	29.994	29.6
50	32.120	32.11	3.2005	3.17	32.572	32.8
45	32.287		3.3670		33.946	
40	32.459	32.45	3.5395	3.53	35.309	36.3
35	32.640		3.7203		36.747	
30	32.827	32.84	3.9071	3.92	38.204	39.8
25	33.022		4.1020		39.642	
24	33.062		4.1418		39.940	
23	33.102		4.1816		40.234	
22	33.142		4.2221		40.528	
21	33.183		4.2632		40.821	
20	33.224	33.25	4.3036	4.33	41.091	42.8
19	33.265		4.3454		41.383	
18	33.306		4.3865		41.672	
17	33.348	33.38	4.4283	4.44	41.960	
16	33.391		4.4707		42.243	
15	33.433		4.5131		42.578	
14	33.475		4.5554		42.776	
13	33.518		4.5984		43.046	
12	33.562		4.6421		43.301	
11	33.605		4.6850		43.540	
10	33.649		4.7292		43.756	
9	33.692		4.7726		43.939	
8	33.736		4.8165		44.069	
7	33.781		4.8609		44.114	
6	33.825		4.9049		44.008	
5	33.868		4.9484		43.610	

[a] Calculated.
[b] Measured; smoothed data of Ref. 6.
[c] Deduced from data.
[d] Derived from the melting pressure data by the experimental workers of Ref. 6.

(±0.03 atm), it is seen that the calculated melting pressures and pressure changes are in agreement with the experimental values, as pointed out by Scribner *et al.*[6] It should, however, be stressed that this agreement between the theoretical and experimental melting-pressure lines of

He^3 is semiquantitative. A more critical comparison of the highly accurate melting-pressure changes with those derived from Eq. (15) is not possible at present.

The last two columns of Table I refer to the melting-pressure derivatives. The calculated ones, $(dP_M/dT)^{(a)}$, result from Eq. (11) while the $(dP_M/dT)^{(d)}$ values have been deduced from experiment.[6] It is not clear at the present time if these deduced derivatives resulted from the accurately measured melting-pressure changes or the less direct melting pressures. As far as the theory is concerned, the melting-pressure derivative is a basic theoretical quantity while experimental derivatives appear to be indirect, and necessarily less accurate than the pressure changes that were actually measured. With this point clearly in mind, there is acceptable agreement between the theoretical and empirical melting pressure derivatives according to Table I.

We give in Table II the theoretical melting-pressure derivatives dP_M/dT and melting-pressure changes $P_M(T) - P_M(T_\gamma)$ for a reference temperature T_γ of 5 m°K, where $P_M(T_\gamma)$ is 33.868 atm by Table I. The temperature range of Table II extends down to our estimated transition temperature of the solid, $T_0 = 2.04$ m°K. Over this range and as shown in Sec. III, below T_0, analytical expressions are available. At $T_0 \leq T \leq 5$ m°K, these approximations, Eqs. (14) and (15), give dP_M/dT and $P_M(T) - P_M(T_\gamma)$. Table II indicates that the variations of these quantities become smaller and smaller and that the temperature resolution of a He^3 melting-pressure thermometer would decrease at very low temperatures approaching T_0. On the assumption that a pressure resolution of $\sim 3\times 10^{-5}$ atm, which was achieved by Scribner *et al.*[6] in

TABLE II. Calculated melting properties of He^3 at the approaches of the spin-ordering temperature T_0 of the solid.

T m°K	$[P_M(T) - P_M(T_\gamma)]$[a] atm	$(-)\ (dP_M/dT)$ atm/°K
4.80	0.00871	43.464
4.60	0.01738	43.297
4.40	0.02602	43.096
4.20	0.03462	42.854
4.00	0.04316	42.561
3.80	0.05164	42.206
3.60	0.06004	41.773
3.40	0.06834	41.241
3.20	0.07653	40.582
3.00	0.08456	39.755
2.90	0.08851	39.261
2.80	0.09241	38.702
2.70	0.09625	38.066
2.60	0.1000	37.337
2.50	0.1037	36.497
2.45	0.1055	36.028
2.40	0.1073	35.522
2.35	0.1091	34.973
2.30	0.1108	34.378
2.25	0.1125	33.731
2.20	0.1142	33.023
2.18	0.1148	32.722
2.16	0.1155	32.409
2.14	0.1161	32.084
2.12	0.1168	31.746
2.10	0.1174	31.395
2.09	0.1177	31.214
2.08	0.1180	31.030
2.07	0.1183	30.841
2.06	0.1186	30.649
2.05	0.1189	30.453
2.04	0.11926	30.252

[a] Reference temperature T_γ is 5.0 m°K.

pressure-change measurements can still be maintained at the very low temperatures, the corresponding temperature resolution may reach (by Table II) about 10^{-3} m°K near the spin-ordering temperature. The loss of resolution will become pronounced below the spin-ordering temperature, as shown in Sec. III.

III. MELTING OF SOLID He^3 BELOW ITS SPIN-ORDERING TEMPERATURE

The infinite series in Eq. (3), which gives an exact representation of the solid-model entropy in ascending powers of $|J_M|/kT$, is a high-temperature expression. The calculated entropies become less accurate the closer T gets to T_0, the here-assumed antiferromagnetic spin-ordering temperature at melting. Since the latter is estimated to be somewhat less than $3|J_M|/k$ by (16), the entropy-series expansion parameter is about $\frac{1}{3}$, so that the truncated series (3) may still approximate the entropy $S_+(T_0)$ on the paramagnetic side of the transition temperature. However, using the entropy (3) is equivalent to omitting all critical aspects of the transformation which, if present, will give rise to an entropy $S_+(T_0)_{cr}$ that is somewhat different from the one resulting from (3). The critical behavior is reasonably expected to be restricted to a rather small temperature interval $|T - T_0|$ around T_0, such as

$$|T - T_0| \lesssim (T_0/100) \sim 0.02 \text{ m°K} \quad . \tag{18}$$

To obtain the melting properties at $T < T_0$, the thermal behavior of the liquid and the solid must be known below the assumed antiferromagnetic spin-ordering temperature of the solid. In contrast with the paramagnetic range, the theoretical representation of the spin system of the solid below T_0 is not as satisfactory. There is presently no proof that the exact high-temperature formalism, $T > T_0$, resulting from the exchange-coupling scheme, is indeed valid in paramagnetic solid He^3. The temperature range explored by Panczyk *et al.*[2] cannot be used to verify the theoretical model even to within the first term beyond the asymptotic term, in the truncated series representation of the isochores of the paramagnetic solid.

The theoretical model to be used here for the spin system of melting solid He^3 below its transition temperature must be modified so its thermal properties conform to those imposed by the exact theoretical model of the paramagnetic solid. These requirements are contained in the following relations:

$$P_{M-}(T_0) = P_{M+}(T_0) \quad , \tag{19}$$

$$\lim_{T \to T_{0-}} \frac{dP_{M-}}{dT} = \lim_{T \to T_{0+}} \frac{dP_{M+}}{dT} \quad . \tag{20}$$

These relations state that the melting pressure and its temperature derivative are continuous at the transition temperature T_0. This is equivalent to stating that the spin-ordering transformation in the solid at melting is a higher-order phase change. Equation (11) combined with (20) requires the continuity of entropy and volume of the solid at T_0 or

$$S_{s,M-}(T_0) = S_{s,M+}(T_0) \quad , \tag{21}$$

$$V_{s,M-}(T_0) = V_{s,M+}(T_0) \quad , \tag{22}$$

since the liquid at melting exhibits no phase transformation in the present theory.

We have chosen to use the asymptotic molecular-field-theory model to describe the antiferromagnetic solid. If the solid at melting turned out to be ferromagnetic, the same model would apply with similar limitations below its ferromagnetic Curie point, which, by (16) is estimated to be at 1.85 m°K. We will indicate only the relevant thermal properties of the model.[9] The energy can be expressed in terms of the relative sublattice magnetization $\sigma(T)/\sigma_0$, $\sigma(T)$ and σ_0 being the magnetic moment per sublattice at temperature T and the absolute zero, respectively. The quantity σ_0 is thus the saturation moment on one of the two sublattices or

$$U_\sigma(\tau)/R = -\tfrac{1}{2}T_0[\sigma(\tau)/\sigma_0]^2, \tag{23}$$

$$\text{where} \quad \sigma(T)/\sigma_0 = \tanh\{[\sigma(\tau)/\sigma_0](1/\tau)\}, \tag{24}$$

$$\tau = T/T_0 \quad .$$

The limiting values of the relative magnetization are

$$\begin{aligned} &\sigma(\tau)/\sigma_0 = 0, \quad \tau = 1 \ ; \\ &\sigma(\tau)/\sigma_0 = 1, \quad \tau = 0 \ . \end{aligned} \tag{25}$$

According to (24), the latter limit is being approached as

$$\lim_{\tau \to 0} \sigma(\tau)/\sigma_0 = 1 - 2e^{-2/\tau} \quad , \tag{26}$$

which will be used later. The heat capacity is given as

$$\begin{aligned} C_\sigma(\tau)/R &= y^2[(\cosh y)^2 - (1/\tau)]^{-1} \quad , \\ y &= [\sigma(\tau)/\sigma_0](1/\tau) \\ &= \operatorname{arctanh}[\sigma(\tau)/\sigma_0] \quad , \end{aligned} \tag{27}$$

and the entropy as

$$S_\sigma(\tau)/R = \ln(2\cosh y) - y\tanh y \quad . \tag{28}$$

Since this asymptotic model acquires the full entropy of $R\ln 2$ at T_0, the continuity condition (21) requires the entropy of the solid below T_0 to be

$$S_-(\tau) = [S_+(T_0)/R\ln 2]S_\sigma(\tau) \quad , \tag{29}$$

$$\text{with} \quad S_+(T_0)/R = \ln 2 - 3\sum_{n=0}(-)^n \frac{c_n}{n+2}(x_0)^{n+2}, \tag{30}$$

$$x_0 = |J_M|kT_0 .$$

To the approximation of the presently known coefficients c_n as well as the empirically estimated value of T_0 [by (16)], one obtains

$$S_+(T_0)/R = 0.4518 \quad . \tag{31}$$

As noted above, we disregard any critical behavior that might be present. Hence, even if the models in both the paramagnetic and spin-ordering temperature ranges were justified, the present treatment would break down within 0.02 m°K of T_0, as estimated in Eq. (18).

The entropy (29) yields the corresponding heat capacity

$$C_-(\tau) = [S_+(T_0)/R\ln 2]C_\sigma(\tau) \quad , \tag{32}$$

with $C_\sigma(\tau)$ given by (27). Finally the energy $U_\sigma(\tau)$ [Eq. (23)] is to be modified according to

$$U_-(\tau) = [S_+(T_0)/R\ln 2]U_\sigma(\tau) \quad . \tag{33}$$

The present treatment of solid He^3 in its spin-ordering range requires two parameters T_0 and $S_+(T_0)$. In the paramagnetic range, there are also two empirical parameters in the formalism, the average $|J_M|$ value and the empirical factor $\tau(A)$, which give T_0 as a function of $|J_M|$ [Eq. (16)]. As emphasized already, the parameter $\tau(A)$ has no theoretical significance at the present time. At high temperature, the infinite series representation of the thermal properties of the paramagnetic exchange-coupled system does not connect the spin-ordering temperature T_0 with the exchange energy parameter $|J|$.

The omission of the possible critical behavior of the solid around T_0 is equivalent to observing the thermal properties of the solid or the melting process with poor temperature resolution. If the resolution is some low multiple of 0.01 m°K, the critical behavior reduces to a λ-type transition where the heat capacity exhibits a finite discontinuity across T_0. One aspect of the critical behavior is expressed by the condition

$$\lim_{T\to T_{0-}} \frac{dS_-}{dT} = \lim_{T\to T_{0+}} \frac{dS_+}{dT}$$

$$= -+(\infty) \quad , \tag{34}$$

where both branches of the entropy S_- and S_+ would join with positive infinite temperature derivatives or the heat-capacity branches would tend to infinity at T_0. Correspondingly, the two branches of the melting-pressure derivative dP_M/dT would join with negative infinite temperature slopes. Indeed, by Eq. (6), and assuming a temperature-independent volume change at melting ΔV_M, one has

$$\frac{d^2P_M}{dT^2} = \frac{1}{T\Delta V_M}\left(C_{L,M} - C_{s,M}\right), \tag{35}$$

and with (34)

$$\lim_{T\to T_{0-}} \frac{d^2P_{M-}}{dT^2} = \lim_{T\to T_{0+}} \frac{d^2P_{M+}}{dT^2}$$

$$= -- (\infty) \quad . \tag{36}$$

Under poor temperature resolution, the melting-pressure derivative has an angular point at T_0, and its temperature slope exhibits a λ-type jump,

$$\Delta\frac{d^2P_M}{dT^2} = \left(\frac{d^2P_{M+}}{dT^2}\right)_{T_0} - \left(\frac{d^2P_{M-}}{dT^2}\right)_{T_0}$$

$$= (-)(1/T_0\Delta V_M)[C_{s,M+}(T_0) - C_{s,M-}(T_0)]$$

$$= -(1/T_0\Delta V_M)\Delta[C_{s,M}(T_0)] \quad . \tag{37}$$

To the approximation of the present treatment,

$$\lim_{T\to T_{0-}} C_{s,M-}/R = (S_+(T_0)/R\ln 2)[C_\sigma(T_0)/R]$$

$$= \tfrac{3}{2}(S_+(T_0)/R\ln 2)$$

$$= 0.9777 \quad , \tag{38}$$

according to the limit $\frac{3}{2}$ of $C_\sigma(T_0)/R$ and the numerical value of $S_+(T_0)/R$ given by (31). With the entropy given by Eq. (3), one obtains, reverting to the heat-capacity series from Eq. (3) and using (16):

$$\lim_{T\to T_0} C_{s,M+}(T_0)/R = 0.6138 \quad , \tag{39}$$

which corresponds to a heat-capacity jump across T_0,

$$\Delta C_{s,M}(T_0) = -0.3639R \ . \qquad (40)$$

With poor temperature resolution, an actual measurement of this jump should yield a value in satisfactory agreement with (40), within the limits of the models used here.

The formalism of the model given above enables one to obtain the melting-pressure equation of He^3 at $T \leq T_0$. The limitations of the model should always be kept in mind.

Instead of going directly to an analysis of the melting process of He^3 at very low temperatures, it is useful to digress and consider a problem which is analogous to the He^3 problem at hand.

Given a first-order phase transformation wherein one of the two phases in equilibrium along the phase-boundary line undergoes a second- or higher-order phase change, is it possible to locate – at least in a semiquantitative way – the transformation temperature of this higher-order phase change through experimental investigations of the pressure-boundary line? Clearly, this problem relates to the location of the spin-ordering temperature through measurements of the melting properties of He^3, assuming, of course, that very low temperatures can be reached.

The entropy and volume of the phase undergoing the higher-order transformation remain continuous at this transition temperature. Consequently, the boundary line of the first-order phase change will be modified only in the second temperature derivative. Rewriting (6) in the somewhat more general form,

$$\frac{dP}{dT} = (S_{\rm I} - S_{\rm II})/(V_{\rm I} - V_{\rm II}) \ , \qquad (41)$$

where all quantities refer to the phase-boundary line, we see that the effect of the higher-order phase change is to modify the shape of the temperature derivative of dP/dT through

$$\frac{d^2P}{dT^2} = \frac{1}{T(V_{\rm I} - V_{\rm II})}\left[(C_{\rm I} - C_{\rm II}) - T\left(\frac{dP}{dT}\right)\left(\frac{d}{dT}\right)(V_{\rm I} - V_{\rm II})\right] . \qquad (42)$$

In the case of He^3, if melting-pressure derivatives could be measured around T_0, the low-temperature resolution measurements should yield these derivatives with an angular point at T_0, enabling one in principle to locate T_0. The jump at T_0 in the second temperature derivative of the melting pressure of He^3 is given by (37) through (40), on the assumption of a temperature-independent ΔV_M. The negative melting-pressure derivative of He^3 is steeper on the low-temperature side of T_0 than on its high-temperature side. The jump $\Delta(d^2P_M/dT^2)$ is thus positive by (37) and (40), in the above treatment. The λ discontinuity in the solid heat capacity has its sign inverted in the jump of the second temperature derivative of the melting pressure across T_0. It is realized that measurements of melting-pressure derivatives at such very low temperatures may be quite laborious. Still, these appear to be less laborious than heat-capacity measurements. It should be noted that derivative measurements of low precision may not be very effective in locating the angular point of dP_M/dT.

It seems interesting to review briefly these derivatives in the vapor-liquid and liquid-solid equilibrium of He^4 near their λ points.

In the vapor-liquid transformation near $T_{\lambda,\,\rm sat}$ at saturation, (I) and (II) in Eq. (41) refer to the vapor and liquid phases. Here, $V_{\rm I} \gg V_{\rm II}$ and $V_{\rm I}^{-1}(dV_{\rm I}/dT)$, the expansion coefficient of the vapor along the saturation line $P_{\rm sat}(T)$, is negative and very large. The positive contribution of the vapor phase to the product inside the brackets on the right-hand side of (42) completely swamps the increasingly large heat capacity $C_{\rm II}$ of the liquid at the approaches of T_λ, this heat capacity being affected by a negative sign there. It is only at temperatures extremely close to the λ point that $C_{\rm II}$ could cause the second temperature derivative of the vapor pressure $P_{\rm sat}(T)$ to become negative over an extremely small temperature range on both sides of T_λ. Actually this interval, $|T_\lambda - T|$, may fall within the range of temperature fluctuations for any reasonable sample volume of He^4 which would exclude the actual observation of an anomalously large temperature slope of the vapor-pressure derivative arising from the heat-capacity anomaly of the liquid phase at its λ point. An elementary calculation yields explicitly with (42)

$$\frac{d^2P_{\rm sat}}{dT^2} \approx \frac{R}{T(V_{\rm vap} - V_L)}\left[\frac{C_{\rm vap} - C_L}{R} + \frac{L}{RT}\left(\frac{L}{RT} - 1\right) + \frac{L}{RV_{\rm vap}}\frac{dV_L}{dT}\right] \ , \qquad (43)$$

where L stands for the latent heat of vaporization, with the subscript L referring to the liquid phase. Around $T_{\lambda,\,\rm sat}$, $(L/RT) \gg 1$, so that the second term inside the braces completely dominates the first and last terms, with the exception of an extremely small temperature interval around $T_{\lambda,\,\rm sat}$. The large negative terms on the right-hand side of (43) arising from the λ transformation of the liquid near $T_{\lambda,\,\rm sat}$ are

$$-\left(C_L + \frac{L}{V_{\rm vap}}\left|\frac{dV_L}{dT}\right|\right).$$

Here, the very large vapor volume V_{vap} around T_λ renders insignificant the large value of $|dV_L/dT|$ near $T_{\lambda,\,sat}$, leaving only C_L to effect a change in the temperature slope of dP_{sat}/dT around $T_{\lambda,\,sat}$. This it cannot do because of the negative and very large expansion coefficient $T^{-1}[1-(L/RT)]$ of the vapor along the saturation line at these temperatures. Hence, the vapor-pressure curve of He^4 remains concave upward, toward increasing pressures, in spite of the modifying influence of the liquid around its higher-order transformation point $T_{\lambda,\,sat}$.

The situation is entirely different along the melting-pressure line of He^4 around the λ point $T_{\lambda,M}$. Here, one has

$$V_{L,M} \gtrsim V_{s,M}\ ;\quad C_{L,M} \gg C_{s,M}\ ;$$

$$S_{L,M} \gg S_{s,M}\ ;\quad |dV_{L,M}/dT| \gg dV_{s,M}/dT\ .$$

Hence, around $T_{\lambda,M}$ Eq. (42) yields

$$\frac{d^2P_M}{dT^2} \sim \frac{1}{T(V_{L,M}-V_{s,M})} \times \left\{C_{L,M} - \left[\frac{TS_{L,M}}{(V_{L,M}-V_{s,M})}\right]\left(\frac{dV_{L,M}}{dT}\right)\right\}, \quad (44)$$

where

$$\frac{dV_{L,M}}{dT} = \left(\frac{\partial V_{L,M}}{\partial T}\right)_p - V_{L,M}\chi_{T,M}\left(\frac{dP_M}{dT}\right) < 0 \quad (45)$$

Both terms on the right-hand side are negative since the liquid has a large negative isobaric expansion coefficient near $T_{\lambda,M}$, and the derivative (dPM/dT) is positive around $T_{\lambda,M}$. The quantity $\chi_{T,M}$ is the isothermal compressibility coefficient of the liquid at melting. Since the volume change at melting, ΔV_M or $V_{L,M}-V_{s,M}$, is positive around $T_{\lambda,M}$, both terms inside the curly brackets on the right-hand side of (44) are positive. With the rapid increase of these terms at the approaches of $T_{\lambda,M}$, the second temperature derivative of the melting pressure increases rapidly, causing the melting-pressure derivative dP_M/dT to develop anomalously large temperature slopes as $T_{\lambda,M}$ is being approached either from below or from above. We see then the feasibility of locating the transition temperature $T_{\lambda,M}$ through direct measurements of the melting-pressure derivatives, but not of the melting pressures alone.

Thus, given the phase-boundary line of a first-order phase transition wherein one of the two phases at equilibrium undergoes a higher-order transformation at a point on the phase-boundary line, as long as the phase that is free of the higher-order transformation remains normal with respect to its thermal properties, the pressure-boundary line will be perturbed by the higher-order transformation of the other phase. This is the case with the melting processes of He^3 and He^4, where this perturbation might be used to locate the temperature of the higher-order phase change. If, however, the phase that is free of the higher-order transformation is thermally anomalous along the pressure-boundary line, its behavior may mask any modification of the boundary line due to the higher-order transformation of the other phase. This is the situation along the vapor-pressure line of He^4 around $T_{\lambda,\,sat}$.

The hcp-bcc transformation of He^3 was studied by us recently[1] in the paramagnetic ranges of the two structures and represents a situation where the pressure phase-boundary line separates two phases which are intrinsically anomalous, both of which undergo spin-ordering transformations at different temperatures.

We return now to melting He^3. As noted in connection with (16) and (17), the locus of spin-ordering temperatures of the bcc solid He^3, $T_0(P)$ ends on the melting line at $T_0(P_M)$. A discussion of this locus will be the subject of later work.

We consider now the analytical representation of the melting pressure of He^3 at $T < T_0$. Within the limitations of the approach developed above, one obtains

$$\frac{dP_{M-}}{dT} = \left(\frac{R}{\Delta V_M}\right)\left\{\gamma T - \left[\frac{S_+(T_0)}{R\ln 2}\right]\left[\frac{S_\sigma(T)}{R}\right]\right\}, \quad (46)$$

assuming ΔV_M to be independent of the temperature and S_σ to be given by (28). It is useful to rewrite the latter, with (24), as

$$S_\sigma(T)/R = \ln\{2/[1-(\sigma/\sigma_0)^2]^{1/2}\} - (\sigma/\sigma_0)^2(1/\tau)\ . \quad (47)$$

One then obtains, with (46),

$$P_{M-}(T_0) - P_{M-}(T) = \int_T^{T_0}\left(\frac{dP_{M-}}{dT}\right)dT = (R/\Delta V_m)\{\tfrac{1}{2}\gamma(T_0^2 - T^2) - [S_+(T_0)/R\ln 2] \times \int_T^{T_0}[S_\sigma(T)/R]\,dT\}. \quad (48)$$

The term $I_\sigma(T_0, T)$ containing the integral inside the curly brackets is, with (29),

$$I_\sigma(T_0, T) = (1/R)\{[T_0S_-(T_0) - TS_-(T)]$$

$$-[U_-(T_0)-U_-(T)]\} \ , \qquad (49)$$

where, by (33),

$$U_-(T_0)-U_-(T)=\tfrac{1}{2}[T_0S_+(T_0)/\ln 2][\sigma(T)/\sigma_0]^2, \qquad (50)$$

is the magnetic energy difference between the states of temperature T_0 and T, according to (23)–(25). Using the entropy (47), the very low-temperature melting-pressure equation is obtained as

$$P_{M-}(T)-P_{M-}(T_0)=(RT_0/\Delta V_M)([S_+(T_0)/R\ln 2]\times\{\tfrac{1}{2}(\sigma/\sigma_0)^2+(1-\tau)\ln 2+\tfrac{1}{2}\tau\times\ln[1-(\sigma/\sigma_0)^2]\}-\tfrac{1}{2}\gamma T_0(1-\tau^2)) \ . \qquad (51)$$

This shows that the melting pressure continues to increase over the spin-ordering temperature range of the solid. However, this increase is not monotonic since the derivative dP_{M-}/dT [Eq. (46)] has a zero somewhat above 0.52 m°K, below which the entropy at melting of the solid is less than that of the liquid. Below this zero of dP_{M-}/dT, the melting process becomes normal, and the melting pressure approaches from above its limiting value at absolute zero by decreasing very slowly from its extremely flat maximum at the indicated zero of the melting-pressure derivative. Using (26), one finds the exact limiting melting-pressure change at $T<T_0$,

$$\lim_{T\to 0} P_{M-}(T)-P_{M-}(T_0)=(RT_0/\Delta V_M)\times\{[S_+(T_0)/R][1-(2\ln 2)^{-1}]-\tfrac{1}{2}\gamma T_0\}. \qquad (52)$$

With the numerical values of $S_+(T_0)/R$ and γ, as well as the estimated value of T_0, this melting pressure difference is

$$P_{M-}(0)-P_{M-}(T_0)=0.01691 \text{ atm}.$$

The melting-pressure decrease between its maximum and its limit at the absolute zero is about 3.10^{-5} atm, to the approximations of the present numerical calculations. This change is just about equal to the pressure resolution achieved by Scribner *et al.*[6] in their measurements of the melting-pressure variations above about 20 m°K. Let us then assume that some such similar pressure resolution may be reached at the very low temperatures. On the high-temperature side of the melting-pressure maximum, a decrease of about 3.10^{-5} atm is achieved at about 0.67–0.68 m°K. Consequently, from 0.68 m°K to absolute zero, the most accurate current techniques of pressure-change measurements at very low temperatures could not detect any variation of the melting line, and the melting-pressure maximum would escape detection. Assuming that melting He^3 could be cooled to temperatures below 0.65–0.70 m°K, He^3 melting-pressure thermometry would become quite insensitive in this region.

It seems pertinent here to give graphs of the melting-pressure derivatives dP_{M+}/dT and dP_{M-}/dT [Eqs. (11) and (46)], and of the melting-pressure changes $P_M(T)-P_M(T_\gamma)$, T_γ being a reference temperature [Eqs. (12) and (48)]. In Fig. 1, the derivative curve below 10 m °K is shown with an inset referring to the range below 1 m°K. The zero of this derivative at about 0.52 m°K and the extremum at about 0.38 m°K are indicated by arrows. The ordinate scale does not accentuate the break point of dP_M/dT at the spin-ordering temperature estimated to be 2.04 m°K. The change in sign of the curvature of the derivative function across T_0 is clear; dP_{M+}/dT is concave upward and dP_{M-}/dT concave downward. This change in curvature is easily accounted for. Near T_0, one has $C_{s,M}\gg C_{L,M}$, and, by (35),

$$\frac{d^2P_M}{dT^2}=-\frac{C_{s,M}}{T\Delta V_M} \ , \quad T\sim T_0 \ . \qquad (53)$$

Assuming a constant ΔV_M, one has

$$\frac{d^3P_M}{dT^3}=\frac{1}{T\Delta V_M}\left(\frac{C_{s,M}}{T}-\frac{dC_{s,M}}{dT}\right). \qquad (54)$$

In the paramagnetic range of the solid, the heat

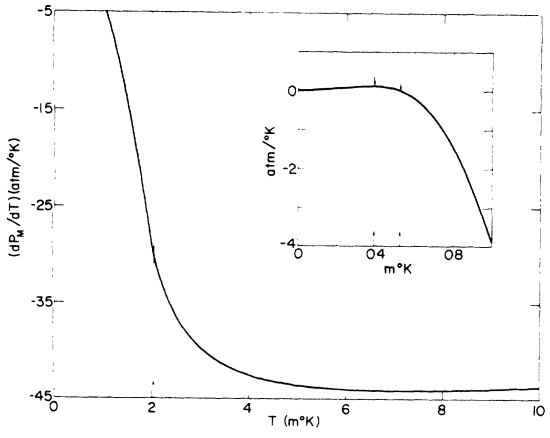

FIG. 1. Temperature derivative of the melting pressure of He^3 at very low temperatures. The inset refers to the lowest temperatures, with the arrows at the temperatures of the inflection point and of the maximum of the melting pressure.

capacity $C_{S,M_+}(T)$ is a decreasing function of T. Both terms inside the parenthesis in (54) are positive, and

$$\frac{d^3P_M}{dT^3}>0, \quad T>T_0 \ . \tag{55}$$

The melting-pressure derivative dP_{M+}/dT is thus concave upward, that is toward increasing values of dP_{M_+}/dT.

In order to see the sign change in curvature below T_0, it is convenient to consider the region near T_0. It is useful to combine (32) with (27), where $(\cosh y)^2$ in the latter is written as $1-(\sigma/\sigma_0)^2$, according to (24), giving

$$C_\sigma/R=(\sigma/\sigma_0)^2[1-(\sigma/\sigma_0)^2]/\ \tau\{\tau-[1-(\sigma/\sigma_0)^2]\} \tag{56}$$

With σ/σ_0 very small near T_0 or $\tau\sim 1$, one finds with (24), expanding its right-hand side to terms in $[\sigma/\sigma_0)1/\tau]^3$,

$$\lim_{\tau\to 1}\ (\sigma/\sigma_0)^2=3(1-\tau) \ . \tag{57}$$

This result is substituted in (56) and with the modified heat-capacity of the model [Eq. (32)] yields

$$\lim_{\tau\to 1}\ C_-/R=[S_+(T_0)/R\ \ln 2]\tfrac{3}{2}(3-2/\tau). \tag{58}$$

The latter then gives, with (54),

$$d^3P_{M-}/dT^3<0, \quad T\lesssim T_0 \tag{59}$$

or the derivative function becomes concave downward, toward decreasing values of dP_{M_-}/dT.

The minimum of dP_{M_+}/dT, that is the higher-temperature inflection point in melting pressure somewhat below 7 m°K, is just barely visible on the ordinate scale of Fig. 1.

Shown in Fig. 2 are the melting-pressure changes $P_M(T)-P_M(T_\gamma)$, T_γ being the reference temperature of 5 m°K, and $0\leq T\leq 5$ m°K. An expanded scale also shows the differences $P_{M_-}(T)-P_M(T_0)$. From Table I, the melting pressure at 5 m°K is 33.868 atm, and the melting pressures at $T<5$ m°K are obtained by simple addition. The melting pressure at T_0 is seen from $P_M(T_\gamma=5$ m°K) and Table II to be 33.987 atm. With the melting-pressure difference $P_M(0)-P_M(T_0)$, Eq. (52) given above, the limiting value of the melting pressure at the absolute zero is just above 34 atm. Various treatments of melting He^3 will yield somewhat different values for the limit $P_M(T\to 0$ °K), but the differences should be small, assuming that the paramagnetic solid is described on the basis of

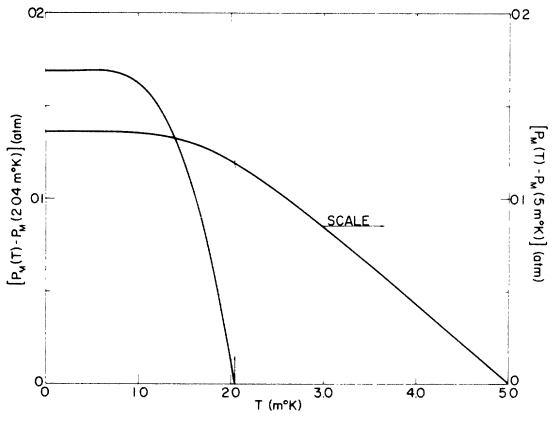

FIG. 2. Melting-pressure variations of He^3 at very low temperatures.

our exchange-coupling model.

The energy difference between melting solid and liquid He^3, in the limit of absolute zero, is then with the limit value $P_M(T\to 0$ °K) of about 34.004 atm, and with the earlier value[7] of ΔV_M of 1.20 cm^3/mole,

$$[E_{S,M}(0)-E_{L,M}(0)]/R=P_M(0)\Delta V_M/R$$
$$=0.497\ °K \ . \tag{60}$$

The following remarks concern the over-all shape of the melting-pressure line. Disregarding the extremely flat maximum of $P_M(T)$ near 0.50 m°K, the calculated shape is similar to that which would be associated with a fictitious paramagnetic solid exhibiting no magnetic transformation, but whose spin system would order in a continuous fashion at the low temperatures. This latter behavior was assumed in our early work[10] on the melting properties of He^3.

This concludes the derivation of the analytical forms of the melting-pressure branches $P_{M+}(T)$, $P_{M-}(T)$, assuming the liquid remains paramagnetic and the solid is in the paramagnetic and spin-ordering temperature ranges. Our main task was to describe formally the melting process within the scope of the models as well as the few empirical parameters entering into the formalism.[11]

We should like to restate the present situation with regard to the comparison of the theoretical and experimental melting properties described in Sec. II. The experimentally explored temperatures are in a range[6] where the character of solid He^3 at melting is asymptotic. The observed, if unexplained, temperature variations of ΔV_M notwithstanding, the above comparison establishes that the theoretical representation of the liquid entropy at melting, $S_{L,M}(T)$, is satisfactory. Determinations of this entropy, above all at the relevant low temperatures,

TABLE III. The coefficients s_σ of the entropy series $\sigma(T_i)$ of the paramagnetic solid, and the coefficients t_λ of the inverted entropy series $x(T_f)$ giving the final temperature T_f of the solid as a function of the initial temperature T_i of the liquid in the adiabatic solidification process of He^3.

s_2	$\frac{3}{2}$	t_1	0.816497
s_3	1.0	t_2	−0.222222
s_4	$\frac{21}{16}$	t_3	−0.0869418
s_5	$-\frac{9}{2}$	t_4	0.479424
s_6	2.656250	t_5	−0.927876
s_7	2.762485	t_6	0.442106
s_8	19.000391	t_7	0.280055
s_9	22.979431	t_8	−2.733392
s_{10}	99.681834	t_9	2.300026

are not available at the present time. The full physical significance of a critical comparison of the calculated and measured melting properties of He^3 can only be found at temperatures much lower than those explored so far.

We now turn toward exploiting the above analysis of $P_M(T)$, assuming tentatively, that later modifications will involve only moderate corrections. In the remaining part of the present work we will investigate two practical consequences of the results obtained above. First, we will extend our earlier work[1] on the production of very low temperatures through adiabatic freezing of He^3, which dealt only with the paramagnetic solid. With the modified molecular-field-theory model of the spin-ordering solid, one obtains an estimate of the theoretical lower limit of the temperatures accessible through this method. Assuming that such cooling is practicable, it will be shown that a He^3 melting-pressure thermometer may be used to establish a thermodynamic temperature scale, extending from about 1.0–1.5 m°K to above 10 m°K. The existence of such thermodynamic temperatures could assist later in reaching the submillidegree range for experimental investigations of high accuracy. This lower range will now be shown to be inaccessible through cooling by adiabatic freezing of He^3.

IV. PRODUCTION OF VERY LOW TEMPERATURES ON ADIABATIC SOLIDIFICATION OF He^3

Our recent work[1] on adiabatic freezing of He^3 was limited to the higher temperatures produced by this cooling method. Calculations of the melting pressure extended only to temperatures $T \geq 5$ m°K, where the solid is still paramagnetic. The complete derivation of the melting-pressure branches, studied in the previous sections, with the branch P-(T) obtained down to absolute zero, enables one to explore the full range of temperatures $T_f(T_i)$ accessible through complete adiabatic solidification of a given sample of liquid He^3 at the initial melting temperature T_i and initial melting pressure $P_M(T_i)$.

Since the models used to describe the thermal properties of the solid are entirely different at $T > T_0$ and $T < T_0$, the calculation of the cooling process in the paramagnetic range of the solid differs in its details from that involving the solid in the spin-ordering range, these states being the final states of the freezing process along adiabatic paths. In the paramagnetic range, we have, rewriting the entropy of the solid given by Eq. (3),

$$\ln 2 - S_{s,M}(T)/R = \sum_{n=0} (-)^n (3c_n/n+2)\,(J_M/kT)^{n+2} \quad , \tag{61}$$

and in the adiabatic process at hand,

$$S_{s,M}(T_f) = S_{L,M}(T_i) \quad , \tag{62}$$

or

$$\ln 2 - S_{L,M}(T_i)/R = \sigma(T_i) = \sum_{\sigma=2} s_\sigma [x(T_f)]^\sigma ,$$
$$x = J_M/kT_f ; \quad \sigma \geq 2 \quad \sigma = n+2 \quad . \tag{63}$$

The latter series connecting T_f and T_i can be inverted to yield

$$x(T_f) = (J_M/kT_f) = \sum_{\lambda=1} t_\lambda [\sigma(T_i)]^{\lambda/2} \quad , \tag{64}$$

where the $x(T_f)$ series starts out with $\sigma(T_i)^{1/2}$ as a consequence of the $\sigma(T_i)$ series starting out with $x(T_f)^2$ in (63).

The series inversion was performed by my colleague, Dr. Paul Stein. The inverted series yields T_f with good accuracy. Table III gives both the coefficients s_σ, $\sigma \geq 2$, which result from the coefficients c_n and the t_λ coefficients of the inverted $x(T_f)$ series. For $\sigma(T_i)$ in (63) and (64), we have used the theoretical expressions of $S_{L,M}(T)$ on which calculations of the melting pressure

were based.

From the entropies $S_{L,M}(T)$ and $S_{S,M}(T)$, one can obtain the final temperature $T_f(T_i)$ indirectly by inverse interpolation in $S_{S,M}(T)$. These interpolated T_f values differ at most by about 0.1 m°K from those resulting from the $x(T_f)$ series (64), this difference occurring only where $S_{S,M}(T_f)$ has a significant second temperature derivative. This was to be expected because of the linear character of the interpolation.

In the spin-ordering range of the solid it is still possible to invert the series

$$\sigma_-(T_i) = \ln 2[1 - S_{L,M}(T_i)/S_+(T_0)]$$
$$= x(T_f)\tanh x(T_f) - \ln\cosh x(T_f)\ ,$$
$$x(T_f) = [\sigma(T_f)/\sigma_0](1/\tau_f); \quad \tau_f = (T_f/T_0)\ . \tag{65}$$

Here use was made of the entropy $S_-(\tau)$ [Eq. (29)], with $S_\sigma(\tau)$ given by (28). The series expansion of $S_-(\tau)$ or $S_\sigma(\tau)$, that is of (65), is only valid at $x > \frac{1}{2}\pi$. In practice, however, a large number of terms of this expansion is required beyond about $x \sim 1$ for satisfactory accuracy. Use of the series inversion together with the inverted series becomes quite tedious. As a consequence, below T_0, the $T_f(T_i)$ values have been derived through inverse interpolation.

The absolute lower-limit temperature $T_{f,\mu}$ attainable with the adiabatic freezing process is, of course $T_{i,\mu}$, the temperature of intersection of the entropy curve $S_{L,M}(T_i)$ and $S_{S,M}(T_f)$, where

$$T_{i,\mu} \equiv T_{f,\mu}\ . \tag{66}$$

This temperature is, of course, the same at which [by Eq. (6)] the melting-pressure derivative vanishes, or where $P_M(T)$ has its maximum, and the second derivative becomes negative. In the present treatment, this is at about 0.524 m°K, as already noted above. The practical lower limit of adiabatic cooling is considerably higher than $T_{f,\mu}$, because the required starting temperature T_i of the liquid is about 10 m°K to produce T_f values below 1.0 m°K. If one rules out cooling by adiabatic demagnetization, then to produce temperatures below 1.0 m°K by adiabatic freezing only, the initial state of the liquid at melting will have to be reached by this same process, thus requiring a two-stage freezing system. Using demagnetization techniques, the required initial state of the liquid at melting, for the adiabatic freezing process, is readily accessible.

Inasmuch as the $Tf(T_i)$ function is of general interest, we give in Fig. 3 the graph of T_f as a function of T_i in the range $T_i < 300$ m°K. The last point of the T_f curve in the inset of Fig. 3 refers to 0.65 m°K, which is associated with a T_i of 2.0 m°K.

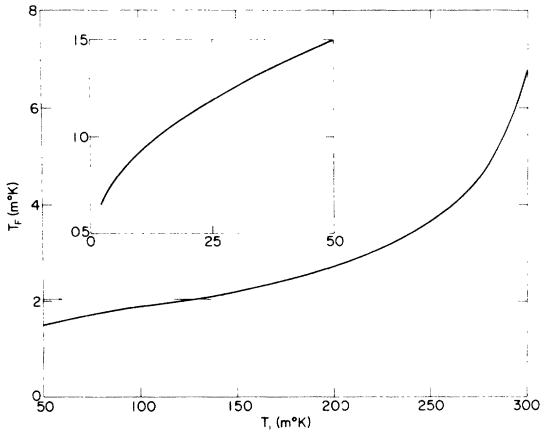

FIG. 3. The function $T_f(T_i)$ characteristic of the cooling on adiabatic freezing of He^3, for $T_i \leq 300$ m°K; inset: $T_i \leq 50$ m°K.

It is seen that as long as $T_i \geq 128$ m°K, the final state of the solid obtained on a complete adiabatic solidification is still in the paramagnetic range, that is,

$$T_f(T_i \geq 128\ \text{m°K}) \geq T_0 = 2.04\ \text{m°K}. \tag{67}$$

It should be clearly kept in mind that the estimated value of T_0 has but indirect connections with either of the assumed exchange-coupling model or with the molecular-field-theory model in the spin-ordering range. Because they are of obvious interest, various calculated properties are given in Tables IV and V, such as $T_f(T_i)$, $S_{L,M}(T_i)$, or $S_{S,M}(T_f)$, the initial melting pressures in the form of the difference $P_M(T_i) - P_M(T_\mu)$, and the total pressure increase $P_M(T_f) - P_M(T_i)$, or compression, needed to freeze adiabatically all of a liquid sample at melting to solid at melting. We have omitted from Table V the initial melting pressures which are available through Tables I and II.

It should be noted that the pressure rate of cooling is given by $(-)(dT/dP_M)$, the negative reciprocal of the melting-pressure derivative over the range $T_{f,\mu} < T < T_\mu$. These rates can be gotten directly from Tables I and II, and Fig. 1. The cooling rates are very large near the extremas T_μ and $T_{f,\mu}$ of the melting line. A minimum is reached near 7 m°K at the inflection point in the melting curve where the cooling rate is somewhat below 23 m°K/atm.

According to the spin-ordering model of the solid used here, the initial temperature of the liquid at melting must be decreased from about 125–130 to 14 m°K or by a factor of about 9 to reduce T_f from 2 to 1 m°K. This illustrates the loss of cooling efficiency below T_0. In models where the temperature rate of decrease of the entropy is faster than in the

molecular-field-theory model, the T_f, to be reached below T_0, will fall even more slowly. In the present model, at $T_f < T_0$, these final temperatures may be lower limits when compared with the final temperatures predicted by other models. This would be expected particularly in the region close to T_0. At T_f values further away from T_0, however, the final temperatures obtained by molecular-field theory, although low, should compare better with the actual values.

We have implied that the final temperatures of interest in the cooling process were at $Tf < 10-15$ m°K. Strictly speaking, this process extends between the two temperatures T_μ and $T_{f,\mu}$, where the entropy curves $S_{L,M}(T)$ and $S_{S,M}(T)$ of the liquid and solid at melting intersect. According to the present calculations, a starting temperature T_i of 300 m°K yields a T_f value somewhat less than 7 m°K. The initial temperature range between 300 and 326 m°K, which approximates T_μ, must then correspond to the T_f range between about 7 m°K and T_μ. The highest T_i value of Table IV at 320 m°K still yields only a T_f value somewhat below 24 m°K. This shows the increasingly steep character of T_f as a function of T_i, as $T_i \to T_\mu$. In the asymptotic range of the solid, the adiabatic condition (62) yields,[1] with (3),

$$\lim_{T_i \to T_\mu} (J_M/kT_f) = (\tfrac{2}{3})^{1/2}[\ln 2 - S_{L,M}(T)/R]^{1/2}. \tag{68}$$

Hence,

$$\lim_{T_f \sim T_i \to T_\mu} \frac{dT_f}{dT_i} = \tfrac{1}{2}[C_{L,M}(T_i)/R] \times \{\ln 2 - [S_{L,M}(T_i)/R]\}^{-1}, \tag{69}$$

which diverges since $S_{L,M}(T_i)/R$ approaches (ln2) as $T_i \to T_\mu$. Equation (68) is the $x(T_f)$ series (64) reduced to its first term, where $\sigma(T_i)$ is close to its vanishing limit at T_μ, the coefficient t_1 of (64) being $(2/3)^{1/2}$.

It is useful to consider the variations of the compression

$$\Delta P_M(T_f, T_i) = P_M(T_f) - P_M(T_i), \tag{70}$$

which must be exerted on the initial sample of the liquid at melting, at T_i and $P_M(T_i)$, to completely solidify it adiabatically and reach the final temperature T_f and melting pressure $P_M(T_f)$. Since T_f depends on T_i, if one eliminates, for instance, T_i between $\Delta P_M(T_f, T_i)$ and $Tf(T_i)$, ΔP_M becomes a unique function of T_f. Since T_i and T_f are identical at T_μ and $T_{f,\mu}$, ΔP_M vanishes identically at these two temperatures. Further, since ΔP_M is always positive between its two zeros at T_μ and $T_{f,\mu}$, it must have at least one maximum. This occurs at T_i close to 280 m°K or T_f close to 5 m°K.

In Sec. V, we turn to the discussion of additional aspects of the cooling process on adiabatic freezing of He^3.

V. MELTING He^3 AS A THERMOMETRIC SYSTEM AT LOW AND VERY LOW TEMPERATURES

We propose to show that melting He^3 might serve as a thermometric system. Furthermore, this same system may help to establish a thermodynamic temperature standard at very low temperatures, from 1.5 m°K upward, where temperature measurements appear to be suspect and limit the accuracy of experimental investigations.

To use He^3 as a thermometric system, one needs to know the unique functional connection $P_M(T)$. This connection appears to be well established at $T \gtrsim 20$ m°K by the accurate results of Scribner *et al.*[6] For thermometric purposes, these pioneering data should be confirmed by independent groups of investigators. Melting He^3 is even now almost usable as a thermometer overlapping the He^3 vapor-pressure thermometer, offering a temperature standard down to 20 m°K. The present problem is to extend this temperature range to much lower temperatures. This extension will also be of thermodynamic character, provided that over this additional range only properties relevant to the thermodynamic variables of state of He^3 are involved in the temperature determinations.

Before entering into the solution of this problem, let us reconsider the limitations which presently concern He^3 melting-pressure thermometry at very low temperature. As discussed in Sec. II, the comparison of the measured[6] and calculated melting pressures down to about 20 m°K is encouraging. However, a comparison has not been made where spin ordering in the solid phase influences the melting process. As a consequence, the only justification for using the exchange-coupled solid model results from the characteristic $1/T^2$ behavior[1] of the derivative thermal property $(\partial p/\partial T)_V$ of isochores in the low-pressure bcc modification of solid He^3, in the asymptotic temperature range[2] $T \gg T_0(V)$. Further support for the model in the paramagnetic range of the solid comes from the anomalous negative sign of the temperature coefficient of the pressure $(\partial p/\partial T)_V$ associated with the fundamental thermal anomaly of the spin system of the solid. This refers to its decreasing entropy on isothermal volume increase, that is,

$$\left(\frac{\partial S_S}{\partial V}\right)_T = \left(\frac{\partial p}{\partial T}\right)_V < 0. \tag{71}$$

This anomaly extended that of the liquid[10] and was subsequently predicted[12] to reach out to quite high temperatures in the solid. The anomaly was observed recently by Panczyk and Adams[13] to reach, at melting, temperatures of over 100 T_0, where T_0 is the spin-ordering temperature estimated to be somewhat higher than 2 m°K. This is in acceptable agreement with our recent calculation[1] of the crossing of the locus of the vanishing derivatives $(\partial p/\partial T)_V$ or that of the vanishing isobaric volume-expansion coefficients $[V^{-1}(\partial V/\partial T)_p]$ of the solid with the melting line $P_M(T)$.

We will now show that the adiabatic freezing of He^3 is well adapted to the establishment of a thermodynamic temperature standard at very low temperatures. The problem is equivalent to the verification of the theoretical melting-pressure equation $P_M(T)$ at those temperatures. If the theory failed to represent in a satisfactory way the melting pressure at the relevant low temperatures, the possibility still exists for the elaboration of an empirical relationship between melting pressure and temperature.

We shall attempt to verify the melting-pressure line $P_M(T)$ of He^3 at the lowest temperatures with the help of a thermodynamic-state variable other than the temperature. Let then

$$P_M = P_M(T), \tag{72}$$

be the formal functional connection between melting pressure and temperature, as resulting from theory, and let

$$\varphi_M = \varphi_M(T), \tag{73}$$

be another measurable thermal property, along the melting line, belonging either to the solid at melting $\varphi_{S,M}$ or to the liquid at melting $\varphi_{L,M}$. It is reasonable to expect that the elimination of the temperature between (72) and (73) should yield the functions

$$\begin{aligned} P_M^{(S)} &= P_M(\varphi_{S,M}), \\ P_M^{(L)} &= P_M(\varphi_{L,M}), \end{aligned} \tag{74}$$

which are rigorously equivalent to the functional connections (72) and (73). There is no loss of generality on assuming that the inverse functions $\varphi_{S,M}(P_M)$ and $\varphi_{L,M}(P_M)$ are also well defined. In the present problem, the melting pressure of He^3, the entropy of the liquid and solid at melting are all functions of the temperature and the volumes of the individual phases or their differences, and no difficulties are expected in the elimination of the temperature between them. The predicted melting pressure can thus be studied as a function of the entropy without involving the measurements of the temperature over that very low range where it must be determined.

The adiabatic freezing or melting of He^3 now provides a direct approach to the experimental verification or establishment of the melting pressure at the very low temperatures. This approach avoids temperature measurements in the latter verification whose function is to determine the temperatures.

Let T_i, $S_{L,M}(T_i)$, and $P_M(T_i)$ be the state coordinates referring to the liquid at melting, in one particular state. According to the results of the previous sections, these starting coordinates are fairly well known and are subject to future improvement. We will first restrict the discussion to the following initial states of the liquid:

$$\begin{aligned} &T_i \geq 128\text{–}130 \text{ m°K}, \\ &P_M(T_i) - P_M(T_\mu) \leq 1.3056 \text{ atm}, \\ &S_{L,M}(T_i) \geq S_{S,M}(T_0) \simeq 0.452\, R\,. \end{aligned} \tag{75}$$

The final states on adiabatic freezing of all the liquid sample of He^3 in (75) are

$$\begin{aligned} &T_f \geq T_0 = 2.04 \text{ m°K}, \\ &P_M(T_f) - P_M(T_i) = \Delta P_M(T_f, T_i) \geq 3.750 \text{ atm}, \\ &S_{S,M}(T_f) \geq S_{S,M}(T_0)\,. \end{aligned} \tag{76}$$

It is assumed that one can control, at melting, both the initial state of the liquid sample and the final state of the solid sample. In the adiabatic freezing process, the measured quantities are

$$T_i, \quad P_M(T_i) \text{ or } [P_M(T_i) - P_M(T_\mu)], \quad S_{L,M}(T_i),$$

wherein the entropy of the liquid $S_{L,M}$ has been determined through earlier preparatory measurements and $P_M(T_i)$ or $[P_M(T_i) - P_M(T_\mu)]$ through direct measurements of the freezing process. In the adiabatic compression leading to complete freezing of the sample, the entropy in the final state is

$$S_{S,M}(T_f) \equiv S_{L,M}(T_i)\,,$$

and one measures the compression

$$\Delta P_M(T_f, T_i) = \Delta P_M[S_{S,M}(T_f)]$$

$$= \Delta P_M[S_{L,M}(T_i)] \qquad (77)$$

or the functional connection between ΔP_M and the entropy $S_{L,M}$ or $S_{S,M}$. The formalism of the liquid and solid at melting, with their theoretical models used above, renders the algebraic elimination of T between $P_M(T)$ and $S_{S,M}(T)$ or $S_{L,M}(T)$ quite tedious. This elimination appears in Tables IV and V. We show in Fig. 4 the result of this elimination which results in the curve of ΔP_M as a function of $S_{S,M}(T_f)$ or $S_{L,M}(T_i)$. If now the measured ΔP_M values in terms of the known initial coordinates cover satisfactorily the $\Delta P_M(S_{S,M})$ curve, in the range investigated, the melting pressure over that entropy range is verified. The knowledge of $S_{S,M}(T)$ defines the temperatures T_f associated with the chosen initial set of states of the liquid. The set of T_f values so obtained refer to the very low temperatures which we set out to determine, together with the measurements of the melting pressures $P_M(T_f)$.

It hardly needs to be emphasized that, for satisfactory accuracy, the freezing or melting must be closely adiabatic. The use of the exchange-coupled model is the basis of the present theory of melting, complemented by the formal representation of the entropy of the liquid at melting elaborated by us.[1] However, one should clearly keep in mind that the estimated value of the spin-ordering temperature T_0 is not connected with the method just described for the verification of the melting line $P_M(T)$ at the very low temperatures and the determination of these latter temperatures. The temperature T_0 does not affect the calculated melting pressures, the compressions $\Delta P_M(T_f, T_i)$, or the entropy $S_{S,M}(T)$ of the solid in the paramagnetic range. It is worth noting again that all calculated thermal properties of the paramagnetic solid at melting are exact, within the limits of validity of the exchange-coupled model and the limitations arising from the polynomial approximations of the relevant thermal properties. Other limitations arise from the empirical nature of the parameters entering into the calculation; the omission of the possible critical behavior of the solid around T_0 must be remembered also.

It appears justified to now state the following. The procedure elaborated here for the verification of the He^3 melting-pressure line down to very low temperatures, to the upper approaches of the absolute theoretical lower limit $T_{f,\mu}$ of the adiabatic freezing process, yielded an accurate thermodynamic temperature standard down to these very low temperatures. Experimental work at these very low temperatures was impeded in the absence of directly measurable temperatures. The thermodynamic standard realized by He^3 melting-pressure thermometry down to very low temperatures should thus be helpful in experimental investigations in a temperature range where methods of direct temperature measurements were absent heretofore.

We must now consider the case in which the theoretical model of the solid fails to represent in an acceptable way the observed $\Delta P_M(S_{S,M})$ or $\Delta P_M(S_{L,M})$ function, or the measured compressions ΔP_M fail to conform to the graph of Fig. 4. This may arise from some T_f value downward or from a certain $S_{S,M}(T_f)$ value down toward lower entropy values. It should be noted in this connection that the shape of the $\Delta P_M(S_{S,M})$ curve is fixed and is of permanent character and cannot change qualitatively. That is, the region where $S_{S,M} \gtrsim 0.62R$ or $T_f \gtrsim 3.4$ m°K [by Table IV] is well established since T_f is still in the asymptotic range with respect to the J_M/kT_f expansion of the entropy of the solid. The failure of the exchange-coupled model would occur at temperatures below about 3.5 m°K.

Let us assume then that down at temperature T_ρ, the entropy $S_{S,M}(T_\rho)$, the $\Delta P_M(S_{S,M})$ function or $\Delta P_M(T)$ and hence $P_M(T)$ have been verified with acceptable accuracy. The calculated melting properties may start deviating from the measured ones at $T < T_\rho$. The measurements of $\Delta P_M(S_{S,M})$ and of $S_{S,M}$ may proceed as at $T > T_\rho$, or $S_{S,M} > S_{S,M}(T_\rho)$. The empirical connection $\Delta P_M(S_{S,M})$ can in principle, be established with accuracy, since $S_{L,M}(T_i)$ (the invariant entropy), $P_M(T_i)$, and T_i are the initial state coordinates, which must be known beforehand. If the observed deviations from the theoretically obtained $\Delta P_M(S_{S,M})$ curve are reasonably small, the temperatures T_f associated with the states of melting He^3 may still be usable. If, however, the theoretical $\Delta P_M(S_{S,M})$ connection becomes a poor approximation to the observed correlations, the empirical establishment of the $P_M(T)$ and $S_{S,M}(T)$ functional relations over the low temperatures becomes extremely laborious as shown by the following considerations.

Let $\Delta P_M^{(1)}$, $S_{S,M}^{(1)}$, and $\Delta P_M^{(2)}$, $S_{S,M}^{(2)}$ be two states below our defined reference state $[\Delta P_M(T\rho), S_{S,M}(T_\rho)]$. Both states (1) and (2) are close to the reference state and let $T_\rho > T^{(1)} > T^{(2)}$. At the very low temperatures, there is a wide range of temperatures $T \gtrsim 1.5$ m°K, where $S_{L,M} \ll S_{S,M}$. One can approximate the melting-pressure derivative

$$\frac{dP_M}{dT} \simeq -\frac{S_{S,M}}{\Delta V_M}, \qquad (78)$$

where ΔV_M is assumed to be constant. If the three states indicated above are close enough, it is possible to obtain a first approximation $T^{(1)}$ of the middle state, according to

TABLE IV. Predicted behavior of He^3 on adiabatic freezing; the solid is paramagnetic.

T_i m°K	$S_{L,M}(T_i)/R$ or $S_{s,M}(T_f)/R$	T_f[a]	T_f[b]	$P_M(T_i)-P_M(T_\mu)$	$P_M(T_f)-P_M(T_i)$
		m°K		atm	
320	0.6918	23.61	23.60	0.000604	4.1517
315	0.6878	12.02	12.02	0.002362	4.6185
310	0.6839	9.18	9.16	0.004119	4.7598
300	0.6757	6.78	6.74	0.01310	4.8574
290	0.66715	5.64	5.57	0.02756	4.8932
280	0.6583	4.84	4.84	0.04885	4.90635[c]
270	0.6490	4.33	4.33	0.07561	4.9017
260	0.6393	3.95	3.95	0.1092	4.8845
250	0.6299	3.66	3.66	0.1490	4.8568
240	0.6193	3.41	3.41	0.1962	4.8200
230	0.6081	3.20	3.20	0.2503	4.7746
220	0.59635	3.02	3.02	0.3127	4.7196
210	0.5839	2.86	2.86	0.3832	4.6554
200	0.5715	2.72	2.72	0.4619	4.5818
190	0.5576	2.60	2.60	0.5495	4.4990
180	0.5427	2.48	2.48	0.6474	4.4054
170	0.5277	2.38	2.38	0.7555	4.3008
160	0.5107	2.29	2.29	0.8746	4.1851
150	0.4935	2.20	2.21	1.0052	4.0573
140	0.4740	2.12	2.13	1.1482	3.9170
130	0.4529	2.04	2.05	1.3056	3.7620

[a] Calculated by inverse interpolation in the entropy $S_{s,M}(T)$.

[b] Calculated through the series inversion of $S_{s,M}(T)$ [Eq. (64)].

[c] The maximum in the compression ΔP_M arises from its dependence either on T_f alone or on T_i alone through the connection $T_f(T_i)$ or $T_i(T_f)$.

$$\Delta T^{(1)} = T_\rho - T^{(1)} \simeq -\tfrac{1}{2}(\Delta V_M)[P_M(T_\rho) - P_M{}^{(2)}]/S_{s,M}{}^{(1)} , \tag{79}$$

by (78). Here,

$$P_M{}^{(2)} = \Delta P_M{}^{(2)} + P_M(T_i{}^{(2)}) , \tag{80}$$

where $T_i{}^{(2)}$ is the initial temperature of the liquid at the melting pressure $P_M(T_i{}^{(2)})$, entropy $S_{L,M}(T_i{}^{(2)})$, which yielded, on adiabatic freezing, the state $(\Delta P_M{}^{(2)}, S_{S,M}{}^{(2)})$. The definition of $P_M{}^{(1)}$ is similar. Measurements relative to a state close to the state $\Delta P_M{}^{(2)}, S_{s,M}{}^{(2)}$ yielding the state $\Delta P_M{}^{(3)}, S_{s,M}{}^{(3)}$ allows one to bracket the new middle state and obtain $T^{(2)}$, with $T^{(1)} > T^{(2)}$ [by use of (79), with the appropriate variables $P_M{}^{(3)}, P_M{}^{(1)}$, and $S_{s,M}{}^{(2)}$]. This procedure can be applied at lower and lower temperatures.

The use of (78) and (79) yields initial approximations to these temperatures $T^{(n)} < T_\rho$. Once these temperatures are established, the liquid entropy at melting can be determined at these temperatures Unless the theoretical entropies of the liquid are usable throughout these very low temperatures, the corrections to the initial temperatures $T^{(n)}$ can be made only when $S_{L,M}(T)$ becomes empirically available there. They can then be used to correct the denominator of (79) by including the small entropies $S_{L,M}(T)$, if such corrections are warranted. The labor involved in this sort of determination of melting pressures and temperatures is extensive. In the absence, however, of even a reasonably approximate theoretical representation of the melting pressures $P_M(T)$ and entropies $S_{s,M}(T)$ at the very low temperatures, this tedious method of obtaining thermodynamic temperature standards cannot be avoided. The differential-difference approach, indicated by (78)–(80), can be replaced by an equivalent integration approach.

Within the limitations of the present calculations, the set of initial states of the liquid defined by

$$T_i \lesssim 128 \text{ m°K}, \quad P_M(T_i) - P_M(T_\mu) \gtrsim 1.3056 \text{ atm}, \quad S_{L,M}(T_i) = S_{s,M}(T_f) \leq S_{s,M}(T_0) , \tag{81}$$

TABLE V. Predicted behavior of He^3 on adiabatic freezing; the solid is in the spin-ordering temperature range.

T_i m°K	$S_{L,M}(T_i)/R$ or $S_{s,M}(t_f)/R$	T_f[a] m°K	$P_M(T_f) - P_M(T_i)$ atm
120	0.4312	1.997	3.5917
110	0.4066	1.944	3.4057
100	0.3810	1.889	3.2027
90	0.3532	1.827	2.9812
80	0.3222	1.7567	2.7400
70	0.2895	1.6801	2.4770
60	0.2543	1.594	2.1907
50	0.2165	1.498	1.8791
45	0.1963	1.444	1.7134
40	0.1763	1.388	1.5415
35	0.1551	1.326	1.3614
30	0.1336	1.260	1.1752
25	0.1122	1.190	0.9808
20	0.09033	1.113	0.7798
19	0.08586	1.096	0.7381
18	0.08138	1.078	0.6971
17	0.07689	1.061	0.6554
16	0.07240	1.042	0.6131
15	0.06709	1.020	0.5708
14	0.06369	1.005	0.5285
13	0.05911	0.985	0.4855
12	0.05458	0.964	0.4420
11	0.05005	0.942	0.3992
10	0.04551	0.919	0.3550
9	0.04097	0.895	0.3117
8	0.03643	0.870	0.2679
7	0.03188	0.842	0.2235
6	0.02733	0.813	0.1795
5	0.02278	0.780	0.1361
4	0.01832	0.745	0.09296
3	0.01374	0.703	0.05159
2	0.00916	0.651	0.01574

[a]Calculated by inverse interpolation in the entropy $S_{s,M}(T)$.

always led to final states, on adiabatic freezing, defined by

$$T_f \leq T_0, \quad P_M(T_f) - P_M(T_i) \leq 3.750 \text{ atm},$$

$$S_{s,M}(T_f) \leq S_{s,M}(T_0). \tag{82}$$

These coordinates refer to states of the solid in the spin-ordering range. The method of verifying the theoretical melting pressure $P_M(T < T_0)$ through measurements of $\Delta P_M(S_{s,M})$ is the same as with the final states $S_{s,M} > S_{s,M}(T_0)$. The $\Delta P_M(S_{s,M})$ function defines the entropy $S_{s,M}(T)$, which in turn defines the final temperatures $T_f(S_{s,M})$ resulting from the theory. To be complete, we include in Figs. 5(a) and 5(b) the graphs of the entropies $S_{s,M}(T)$ and $S_{L,M}(T)$.

If the theory failed to represent the measured ΔP_M values to a satisfactory approximation, the method just discussed for low temperatures $T > T_0$ [Eqs. (78)–(80)] can be used. However, a reference temperature T_ρ must be known at the start. As emphasized above, the theoretical melting pressures in the spin-ordering range are expected to be poorer approximations to the actual values than those referring to the paramagnetic range of the solid.

The temperatures T_f determined through the melting pressures of He^3 may be termed thermodynamic, since the physical properties directly involved refer strictly to the statistical thermodynamics of this element.

It is outside the scope of the present work to consider technical approaches which might evolve in He^3 melting-pressure thermometry. In some cases, melting He^3 might be used as a heat reser-

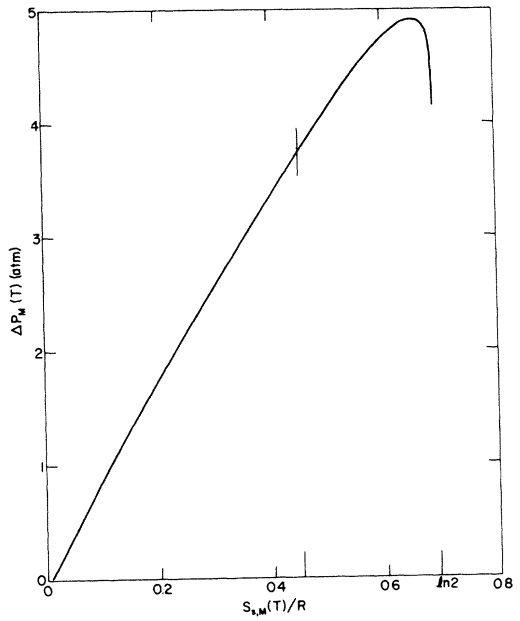

FIG. 4. Calculated adiabatic compression or melting-pressure change, $\Delta P_M(T)$, represented as a function of the entropy $[S_{s,M}(T)/R]$ of the solid produced in the freezing process.

voir or bath. In others, a melting-pressure cell in good thermal contact with the system under investigation might be the thermometer.

We will conclude by stating that the lowest temperatures accessible through adiabatic freezing of He^3 is possibly 1 or 1.5 m°K. To reach fractional and submillidegree temperatures, magnetic cooling must be used at the present time. An improvement of the magnetic technique may arise through the combined use of the method studied in this paper. With magnetic fields of only moderate strength, very large values of the magnetic adiabatic invariant H/T, H being the strength of the applied magnetic field, could be reached. These remarks assume, however, that difficulties in reaching thermal equilibrium in the magnetic techniques are not insurmountable at ultralow temperatures. It seems to us that the thermodynamic very low temperature standard provided by melting He^3 could be helpful in charting the submillidegree temperature range.

ACKNOWLEDGMENTS

Thanks are due Mrs. J. E. Powers, who performed most of the numerical calculations. Mrs. B. E. Powell assisted with graphical work. Dr. Paul Stein cooperated through studying the problems of series inversion, with Myron L. Stein performing the computational work. Last, but not least, I had the good fortune of countless discussions with my colleague and good friend, Dr. Robert L. Mills, on the many aspects of the problems considered in this paper.

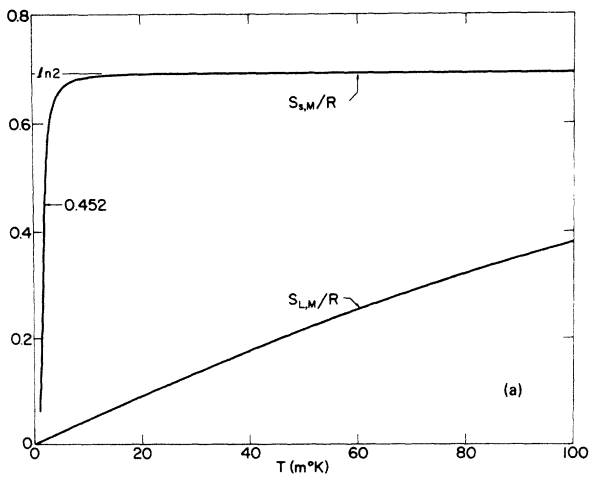

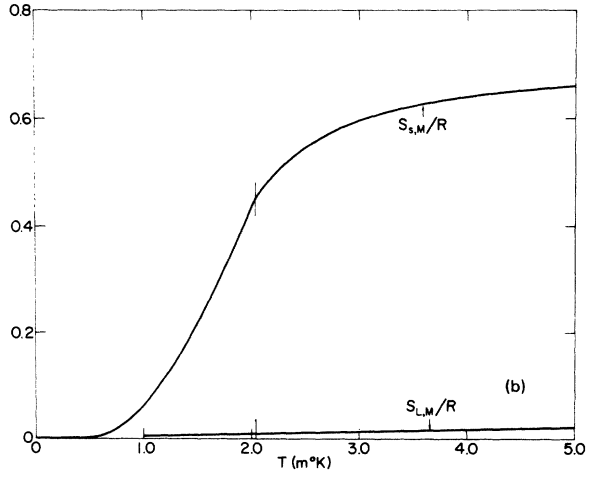

FIG. 5. (a) Theoretical entropy curves $[S_{s,M}(T)/R]$ and $[S_{L,M}(T)/R]$ below 100 m°K. (b) Theoretical entropy curves below 5 m°K; for clarity, the curve of the liquid entropy is stopped at 1 m°K. It intersects the graph of the solid entropy at 0.524 m°K, as stated in the text.

[1]L. Goldstein, Phys. Rev. 159, 120 (1967); 171, 194 (1968); 176, 311 (1968).

[2]M. F. Panczyk, R. A. Scribner, G. C. Straty, and E. D. Adams, Phys. Rev. Letters 19, 1102 (1967).

[3]G. S. Rushbrooke and P. J. Wood, Molecular Phys. 1, 257 (1958); 6, 409 (1963).

[4]G. A. Baker, Jr., H. E. Gilbert, J. Eve, and G. S. Rushbrooke, Phys. Rev. 164, 800 (1967). The coefficients e_n of this reference are connected to the $a_n^{(0)}$ coefficients of our work, the second paper of Ref. 1, and to the coefficients c_n of Ref. 3, according to $c_n = a_n^{(0)} = [(e_{n+2})/3 \times 2^{n+2} \times n!]$.

[5]L. Goldstein, Phys. Rev. 148, 108 (1966).

[6]R. A. Scribner, M. F. Panczyk, and E. D. Adams, Phys. Rev. Letters 21, 427 (1968).

[7]R. L. Mills, E. R. Grilly, and S. G. Sydoriak, Ann. Phys. (N. Y.) 12, 41 (1961).

[8]E. D. Adams and M. F. Panczyk, Bull. Am. Phys. Soc. 13, 1690 (1968).

[9]For recent discussions of this model, cf. A. H. Morrish, The Physical Principles of Magnetism (John Wiley & Sons, Inc., New York, 1965); and J. S. Smart, Effective Field Theories of Magnetism (W. B. Saunders Co., Philadelphia, Pa., 1966).

[10]L. Goldstein, Ann. Phys. (N. Y.) 16, 205 (1962); cf. also L. Goldstein and R. L. Mills, Phys. Rev. 128, 2479 (1962).

[11]J. R. Thompson and H. Meyer, Cryogenics 7, 296 (1966), have produced numerical values of the melting pressure using the same paramagnetic solid model as the one used by us earlier [Ref. 1] and in our present work. Their model in the spin-ordering range was, however, hardly defined. Also, the entropy values of the liquid at melting used by these authors were of strictly empirical origin.

[12]L. Goldstein, Phys. Rev. 133, A52 (1964).

[13]M. F. Panczyk and E. D. Adams, Phys. Rev. 187, (1969).

PHYSICAL REVIEW VOLUME 188, NUMBER 1 5 DECEMBER 1969

Hydrodynamics and Third Sound in Thin He II Films*

D. Bergman†

Institute for Pure and Applied Physical Sciences, University of California, San Diego, La Jolla, California 92037

(Received 8 May 1969; revised manuscript received 20 June 1969)

The linearized hydrodynamic equations of motion for a thin, flat, superfluid helium film are derived in some detail from standard two-fluid hydrodynamics. Interactions of the film with both the He vapor and the substrate which are in contract with it are included and discussed in detail. Boundary conditions for both the film-substrate and film-gas interfaces are derived. It is indicated how one may construct the equations of motion for the entire coupled system (gas-film-substrate). The equations are actually constructed and solved for the case when a certain parameter is small, which includes all the third-sound experiments on unsaturated films. A dispersion equation is found which is exact in the limit of vanishing frequency, and which is eminently suited to describe both the velocity and the attenuation of third sound in the regime of unsaturated films. No hydrodynamic instability is found. Results for the attenuation are shown to be in good agreement with preliminary experiments on unsaturated He films.

I. INTRODUCTION

As a result of increasing interest recently in the properties of third sound in thin He II films,[1-5] we have undertaken to reexamine the theory of that phenomenon with the intention of trying to resolve some difficulties that were present in its original formulation by Atkins.[6] Those difficulties had to do with the theoretical expression for the coefficient of attenuation of third sound, and were of two types: (i) The attenuation became negative for films that were too thin, i.e., it changed into amplification. If this were correct it would imply that the film was then unstable against perturbations of its shape. Such speculations have indeed been made.[4] (ii) Even for thicker films, where this did not happen, the values predicted for the attenuation coefficient were much less than those observed.[1,2] Since the attenuation effects in Atkin's theory[6] arose from the reciprocal processes of evaporation and condensation of He atoms between the film and the gas, we suspected that these processes had not been adequately dealt with in that theory. In this paper, we reformulate the hydro-